

GIS-based Landslide Susceptibility Zoning Using Multi-Criteria Decision-making Method: A Case Study in Binalood Mountains, Iran

Ali Dastranj¹, Hamzeh Noor¹, Ali Bagherian Kalat¹

Date of submission: 16 May. 2021 Date of acceptance: 26 Oct. 2021

Original Article

Abstract

INTRODUCTION: Landslides are one of the recurrent natural problems that are widespread throughout the world, especially in mountainous areas, and cause a significant injury to and loss of human life and damage to properties and infrastructures. This study aimed to assess landslide susceptibility using the analytic hierarchy process (AHP) in Binalood Mountains, Razavi Khorasan Province, Iran.

METHODS: Since the Binalood Mountains range has a high potential for landslides occurrence, the present study went through to map landslide susceptibility. To accomplish this, the AHP method was used, and then, receiver operating characteristic/area under the curves (AUCs) were prepared to evaluate the performance of the susceptibility map. Multiple data, such as lithology, distance to faults, land use, distance to roads, altitude, slope, aspect, stream power index, topographic wetness index, rainfall, distance from rivers, slope length index, and topographic location index, were considered for delineating the landslide susceptibility maps. These thematic layers were assigned suitable weights on the Saaty's scale according to their relative importance in landslide occurrence in the study area. The assigned weights of the thematic layers and their features were subsequently normalized using the AHP technique. Finally, all thematic layers were integrated by a weighted linear combination method in a geographic information system tool to generate landslide susceptibility maps.

FINDINGS: The landslide susceptibility maps are split into five classes, namely very low, low, moderate, high, and very high. The results showed that the geological factor was the most important factor affecting the occurrence of landslides in the study area. Generally, 47.8% of the total area was considered high and very high-risk areas. The prediction accuracy of this map showed the values of AUC equal to 81.7% that showed the AHP model had very good accuracy.

CONCLUSION: Overall, AHP is acceptable for landslide susceptibility mapping in the study area. A landslide susceptibility map is a useful tool to help with land management in landslide-prone areas. The results revealed that the predicted susceptibility levels were found to be in good agreement with the past landslide occurrences. Possibly, this map can be used by the concerned authorities in disaster management planning to prepare rescue routes, service centers, and shelters.

Keywords: AHP Method; Binalood Mountains; Landslide Susceptibility; ROC Curve.

How to cite this article: Dastranj A, Hamzeh N, Bagherian Kalat A. GIS-based Landslide Susceptibility Zoning Using Multi-criteria Decision-making Method: A Case Study in Binalood Mountains, Iran. *Sci J Rescue Relief* 2022; 14(1): 19-29.

Introduction

Landslides are dangerous geological disasters that pose a serious hazard to people's lives and (22) and severe damages to property. The death toll caused

by landslides is high worldwide (7). Due to the large number of deaths caused by landslides throughout the world, it is exigent to predict landslide-prone areas. Although it is impossible to

1- Soil Conservation and Watershed Management Department, Khorasan Razavi Agricultural and Natural Resources Research and Education Center, Mashhad, Iran

Correspondence to: Ali Dastranj, Email: dastranj66@gmail.com

prevent landslide occurrences, disasters can be predicted and remedied using appropriate methods and analysis.

Among various landslide prediction methods, landslide susceptibility mapping (LSM) is an effective land use management technique, which can provide favorable support for land managers in decision-making (9, 22). Landslide hazard and risk assessments start from landslide susceptibility mapping of the territory under investigation (8, 10). Generally, landslide susceptibility is the spatial probability of land sliding in a given area, depending on the combination of various factors, such as geology, land use, land cover, tectonics, slope, and aspect (23). Landslide susceptibility mapping is a helpful tool to predict and locate landslide occurrences. Since the LSM provides valuable information, local governments are inclined to apply it in master planning (1, 6).

The LSM methods have been mainly divided into two groups, namely qualitative and quantitative. Qualitative methods depend on the opinions and judgments of experts, while quantitative methods conduct mathematical analysis and establish a probability statistical model to analyze the relationship between landslide occurrences and influencing factors (21, 22). In this regard, geographic information system (GIS)-based Multi-Criteria Decision Making (MCDM) methods are valuable and ingenious approaches to change either spatial or non-spatial data into desired information that, along with the subjective judgments of decision-makers, would be able to perform in crucial decisions (1, 5). The analytical hierarchy process (AHP) is a semi-quantitative method and is the most prevalent MCDM procedure (1) in which decisions are taken using weights through pairwise relative comparisons without inconsistencies in the decision process (11).

As this research goes through to map landslide susceptibility by applying the AHP method, some previous studies conducted using this method have been mentioned in the following. Kumar et al. (12) used AHP to map landslide susceptibility in Tehrij Reservoir Rim Region, India. Based on the results in their study, 18% of total areas were located in high and very high susceptibility regions. Nguyen et al. (14) applied AHP to generate landslide susceptibility maps in the Chen-Yu-Lan watershed, Taiwan. The validation

of the results by the binary classification method showed that the model had reasonable accuracy. Mandal and Mandal (13) used AHP to LSM in the Lish River basin of eastern Darjeeling Himalaya, India. To validate the results, a success rate curve was developed with the help of landslide susceptibility and cumulative percentage of landslide occurrence, which showed an accuracy level of 89.72%.

As landslides cause a huge loss of human life and property annually all over the world, an accurate assessment of the occurrence of these extreme events is needed. Moreover, even a small increment of the prediction accuracy may control the resulting landslide susceptibility zones. Therefore, much more case studies are required to be conducted to reach a reasonable conclusion. Since the Binalood Mountains range, Razavi Khorasan Province, Iran, has a high potential for landslides occurrence, the present study went through to map landslide susceptibility. Landslide susceptibility is the key component of landslide hazard and risk assessment and in land use planning.

This study discussed landslide susceptibility assessment and mapping using AHP in Binalood Mountains. Binalood Mountains is important due to the existence of communication roads (i.e., roads and national railways) to the city of Mashhad, Iran, development plans, factories and industrial estates, residential areas, gardens, and agricultural lands. Therefore, it is necessary to conduct scientific research on LSM.

Methods

Study Area

The study area is located in the Binalood Mountains part of Razavi Khorasan Province (Figure 1), which covers an area of approximately 3,500 km² with an altitude varying from 1,095 m to 3,298 m above sea level. The slope angles of the area range from 0 to 75°. It lies between 58°38' E and 59°35' E longitude, and 36°1' N and 36°15' N latitude. According to the Iran Meteorological Organization, the study area has a cold and semi-arid climate. The mean annual rainfall is around 320 mm, and the mean annual temperature is 13°C (Zomorodian, 2013). The study area is covered by various types of lithologic formations. The main lithologies are Conglomerate, tuff, slate, phyllite, marlstone, sandstone, shale, grayish limestone, and quaternary terraces (24).

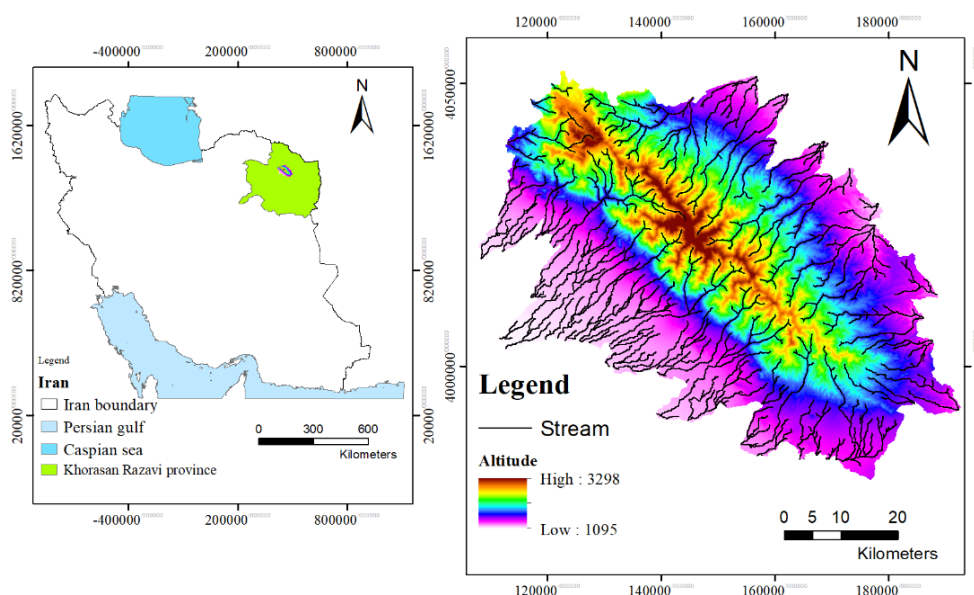


Figure 1. Location map of the study area (Authors)

Methodology

The research aimed to obtain the LSM in Binallod Mountain using the AHP method which had already satisfactory results in analyzing natural phenomena. Landslide susceptibility mapping in the present study was as conducted in the following steps:

Landslide information (landslide inventory map) was collected.

The factors affecting the occurrence of landslides were identified, and then, information related to these factors was gathered, and the effect of each of these factors on the landslide phenomenon was evaluated. The layers of effective parameters were prepared using ArcMap10.5, SAGA, Google Earth, and Arc SWAT.

The preference of different factors on landslide occurrence was determined using the AHP method. The influence weights of variables were calculated.

The influence weight of each layer was multiplied in each parameter using raster calculator tools in the GIS tool. At the next step, landslide susceptibility index (LSI) was calculated weighted arithmetic sum method which can be formulated as given below:

$LSI = \sum \text{weight of factor } (W_j) * \text{weight of factor classes } (W_{ij})$ (1) where W_{ij} denotes the weight of the class of factor J . The LSI map was classified into very low, low, moderate, high, and very high susceptibility classes employing

the natural break classification method in the ArcGIS software.

At the end of this study, a receiver operating characteristic (ROC) curve was used to evaluate the performance of the landslide susceptibility map.

These steps are explained below.

Landslide inventory map

Landslide inventory maps can be prepared either by collecting historical information of individual landslide events or using satellite imageries and aerial photographs coupled with field surveys by the global position system. In the study area, the landslides were identified from aerial photographs of 1964 on a scale of 1:20000 by the General Department of Natural Resources of Razavi Khorasan Province. This map was modified through field surveys and Google Earth images (Figure 2).

Predisposing factors

A landslide is a complex phenomenon that occurs due to several factors (16). The selection of landslide influencing factors has an important impact on the final LSM (15). In this study, 13 landslide influencing factors were considered (Table 1), including lithology, distance to faults, land use, distance to roads, altitude, slope, aspect, stream power index (SPI), topographic wetness index (TWI), rainfall, distance from rivers, slope length index (LS), topographic location index (TPI).

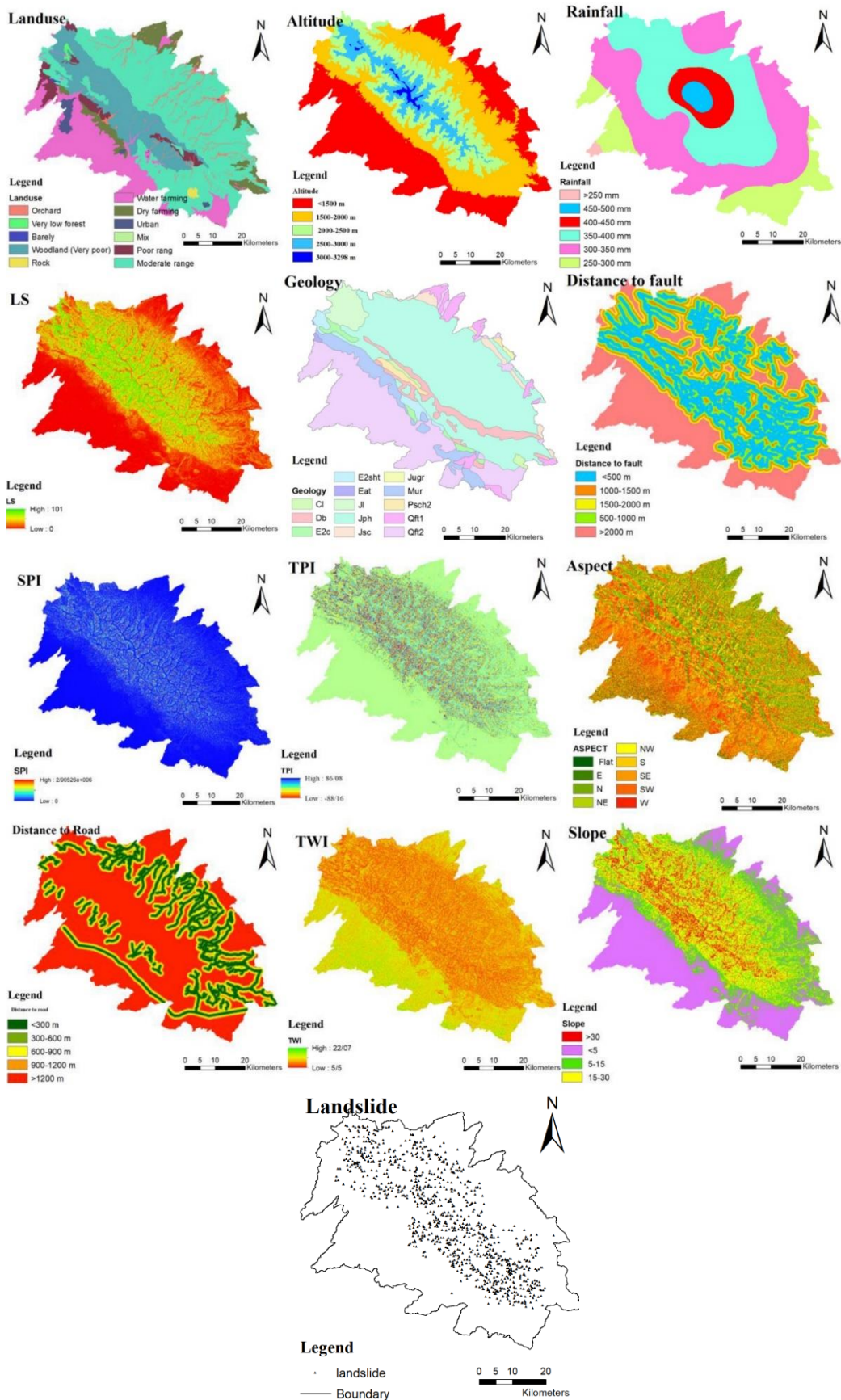


Figure 2. Factors used to identify the landslide susceptible areas in the present study (authors)

Table 1. Causative factors of landslide in the study area

| No | Factor | Description |
|----|----------------------------|--|
| 1 | Lithology | Geology plays a highly important role in landslide susceptibility studies since different lithological classes vary among themselves in terms of mechanical and hydraulic characteristics (18). Rock units in the study area were digitized from geological maps with a 1:100000 scale from the Geological Survey of Iran (Figure 2). |
| 2 | Distance to faults | Faults increase landslide susceptibility because the rocks near a fault are weaker, due to intense shearing (11). Faults were extracted from the geological map of Neishabour, Iran, with a 1:100000 scale. There are several faults in the study area. By increasing the distance from faults, their effect on landslide susceptibility decreases; therefore, a fault buffer map was also generated in ArcGIS (Figure 2). |
| 3 | Land use | Land use is an important factor for landslide susceptibility. This factor has both positive and negative roles in the landslide occurrence. The land cover would cause the slopes to stabilize or may lead the slopes to be unstable (1, 22). In the current study, this layer was prepared from the General Department of Natural Resources of Razavi Khorasan Province, and then, modified using Google Earth images (Figure 2). |
| 4 | Distance to roads | The construction of road activities is cutting the slopes. The natural slopes are disturbed due to these human activities. The slopes near the road are more susceptible to landslide occurrence (16). In this study, the distance of the road map was extracted through Google Earth images; consequently, a buffer map was generated in ArcGIS (Figure 2). |
| 5 | Altitude | Altitude is also a factor that can cause landslides occurrence. The altitude layer was extracted from study area DEM in the ArcGIS software (Figure 2). |
| 6 | Slope | Slope is one of the most important parameters which influences landslide occurrence. The slope angles from 35' to 45' are more susceptible to failure. There are seldom slope failures for the slopes with an angle less than 15' (16). The slope map is extracted from the DEM of the study area (Figure 2). |
| 7 | Aspect | Aspect affects the susceptibility of landslide indirectly or directly. It influences the evaporation and absorption of water (16). The direction of a slope can be related to the causative factors of landslides. In this study, the aspect map was extracted from the DEM of the study area (Figure 2). |
| 8 | Stream Power Index | Stream power index controls the potential erosive power of the overland flow. Therefore, this factor can be considered as one of the factors of landslide occurrence (17). The SPI map was produced using the study area Digital Elevation Model (DEM) in GIS-SAGA software (Figure 2). |
| 9 | Topographic Wetness Index | The topographic wetness index (TWI) has been used to describe the effect of topography on the location and size of saturated source areas of runoff generation (17). It is a commonly used tool to forecast the amount of soil moisture. The TWI layer was produced using study area DEM in GIS-SAGA software (Figure 2). |
| 10 | Rainfall | Rainfall is the most important landslide triggering parameter that increases pore-water pressure and causes soil saturation and runoff through the infiltration of water into the soil (1). In this study, to obtain the rainfall layer, the average annual precipitation data of Razavi Khorasan Province were gathered from the General Department of Natural Resources of Razavi Khorasan Province. Afterward, this layer was extracted in ArcGIS through the Inverse Distance Weighting interpolation method (Figure 2). |
| 11 | Distance to rivers | The distance from rivers is considered a causative factor of landslides occurrence. Run-off of the rivers causes slope failure in the study area (16). Streams may adversely affect stability by eroding the slopes or saturating the lower part of the material. An increase in the distance from rivers causes a decrease in their effect on landslide susceptibility; therefore, a river buffer map was also generated in ArcGIS (Figure 2). |
| 12 | Slope Length | A relationship is relevant between landslides and the SL. It is thought that an increase in the height and SL leads to a growth in slope instability (2). The slope length layer was produced using study area DEM in GIS-SAGA software (Figure 2). |
| 13 | Topographic Position Index | The topographic position index is computed as a difference between the cell elevation and mean elevation of neighboring cells. To categorize existing topographic landforms (i.e., slope, ridge, and valley) specific values of thresholds are needed to be defined (19). Topographic position index was employed in this study to identify ridge, lower flat, valley, and side slope. The topographic position index layer was produced using study area GIS-SAGA software (Figure 2). |

Table 2. Scale of relative importance suggested by Saaty (12)

| Scale | Degree of Preference | Explanation |
|---------|----------------------|---|
| 1 | Equally | Factors inherit equal contribution |
| 3 | Moderately | One factor moderately favors over others |
| 5 | Strongly | Judgment strongly favors over others |
| 7 | Very strongly | One factor very strongly favors over others |
| 9 | Extremely | One factor favors over others in the highest degree |
| 2, 4, 6 | Intermediate | Compensation between weights 1, 3, 5, 7, and 9 |

Analytic hierarchy process method

A nine-point scale, provided by Saaty, is used for the pairwise comparison of causative factors. Table 2 presents the nine points of Saaty’s scale. The AHP consists of three main steps, including generating the pair-wise comparison matrix, computing the weights of the criterion, and estimating the consistency ratio (18). One of the important aspects of the AHP principle is the calculation of consistency index (CI) and consistency ratio (CR). If CR is greater than 0.1, the comparison matrix is inconsistent and should be revised (11).

$$CI = \lambda_{max} - N / (N - 1) \quad (2)$$

$$CR = CI / RI \quad (3)$$

where λ_{max} is the maximum eigenvalue and N is the number of elements present in the row/column of the matrix. In eq. 3, RI stands for random index.

Efficiency of the landslide susceptibility map

The prediction of landslide susceptibility map is usually produced using independent information that is not available for building the model. One of the ways to validate the landslide susceptibility map is the ROC value and the area under the ROC curve (17). In this study, the ROC curve was applied as a worthy tool for appraising the validation of landslide susceptibility maps

derived from the AHP method. The receiver operating characteristic curve is mostly used to show the connection between specificity and sensitivity in a graphical way (1). The area under the curve (AUC) gives a good idea of how well the model performance is and varies from 0.5 to 1. The closeness of AUC values to 1 indicates a better performance of prediction models.

Findings

The present research is based on the use of AHP method for landslide susceptibility map (LSM) in the Binalood Mountains. The preference values for the present study are tabulated in Table 2. The top part of Table 3 is the comparison of causative factors, and the remainder of Table 2 is the comparison of the classes in each factor. These weight values indicate the importance of a class or a factor. According to Table 3, geology is the most important causative factor followed by slope, fault, rainfall, and aspect, while causative factors, such as distance from road and altitude, are less important. Table 3 shows that all CR values are less than 0.1, which demonstrates that the preferences used to produce the comparison matrices were consistent.

Table 3. AHP weights of factors/classes and consistency ratio

| Factors | Classes | Weight | CR |
|--------------|---------------------|--------|------|
| Main factors | Geology | 0.209 | 0.08 |
| | Slope | 0.202 | |
| | Fault | 0.133 | |
| | Rainfall | 0.106 | |
| | Aspect | 0.074 | |
| | TPI | 0.055 | |
| | Topographic indexes | 0.050 | |
| | Distance to river | 0.045 | |
| | Land use | 0.033 | |
| | Altitude | 0.030 | |
| Geology | Road | 0.016 | |
| | Soft rocks | 0.661 | |
| | Loose sediments | 0.231 | |
| | Hard rocks | 0.108 | |

Table 3. Continued

| | | | |
|---------------------|---------------------------|-------|------|
| Rainfall | <250 mm/year | 0.045 | 0.01 |
| | 250-300 mm/year | 0.065 | |
| | 300-350 mm/year | 0.101 | |
| | 350-400 mm/year | 0.161 | |
| | 400-450 mm/year | 0.252 | |
| | 450-500 mm/year | 0.376 | |
| Altitude | <1500 m | 0.046 | 0.05 |
| | 1500-2000 m | 0.107 | |
| | 2000-2500 m | 0.209 | |
| | 2500-3000 m | 0.388 | |
| | >3000 m | 0.251 | |
| Aspect | N | 0.283 | 0.06 |
| | NE | 0.213 | |
| | NW | 0.156 | |
| | E | 0.102 | |
| | SE | 0.072 | |
| | SW | 0.056 | |
| | S | 0.054 | |
| | W | 0.046 | |
| Distance to river | <300 m | 0.502 | 0.04 |
| | 300-600 m | 0.239 | |
| | 600-900 m | 0.127 | |
| | 900-1200 m | 0.079 | |
| | >1200 m | 0.052 | |
| Distance to road | <100 m | 0.441 | 0.03 |
| | 100-200 m | 0.272 | |
| | 200-300 m | 0.138 | |
| | 300-400 m | 0.090 | |
| | >400 m | 0.06 | |
| Land use | Barely | 0.216 | 0.03 |
| | Woodland (very poor) | 0.175 | |
| | Very poor forest | 0.168 | |
| | Poor rang | 0.150 | |
| | Moderate range | 0.136 | |
| | Dry farming | 0.037 | |
| | Mix (dry farming-orchard) | 0.029 | |
| | Orchard | 0.027 | |
| | Water farming | 0.023 | |
| | Rock | 0.02 | |
| Urban | 0.019 | | |
| Slop | <5° | 0.055 | 0.05 |
| | 5-15° | 0.126 | |
| | 15-30° | 0.447 | |
| | >30° | 0.372 | |
| Topographic indexes | SPI | 0.49 | 0.03 |
| | TWI | 0.321 | |
| | LS | 0.189 | |
| Distance to fault | <500 m | 0.43 | 0.01 |
| | 500-1000 m | 0.261 | |
| | 1000-1500 m | 0.163 | |
| | 1500-2000 m | 0.089 | |
| | >2000 m | 0.056 | |

AHP: Analytical hierarchy process; CR: Consistency ratio; TPI: Topographic location index; SPI: Stream power index; TWI: Topographic wetness index; LS: Slope length

Table 4. Area and percent of landslide susceptibility classes

| Susceptibility classes | Area (km ²) | Percent |
|------------------------|-------------------------|---------|
| Very low | 1079.7 | 30.9 |
| Low | 277.9 | 7.9 |
| Moderate | 468.8 | 13.4 |
| High | 979.8 | 28 |
| Very high | 685.6 | 19.8 |

Raster maps of each factor were assigned weight values. The landslide susceptibility index map containing numerical susceptibility information was prepared using eq. 1. In this map, higher LSI values indicated high susceptibility and lower values represented low susceptibility (Figure 4).

Landslide susceptibility index values were found in the range of 0.08-0.43 (Figure 4). Natural break classifier was used to calculate class break values of the continuous LSI map, which is depicted in Figure 4, and accordingly, the LSI map was classified into five categories, namely very high susceptibility, high susceptibility, moderate susceptibility, low susceptibility, and very low susceptibility (Figure 4). It was revealed that 3%, 15%, 25%, 34%, and 23% of the entire area

belonged to very high susceptibility, high susceptibility, moderate susceptibility, low susceptibility, and very low susceptibility classes, respectively (Table 4).

Validation of the landslide susceptibility map

Accuracy of landslide susceptibility map is the capability of a map to delineate landslide-free and landslide-susceptible areas. Validation was performed to obtain the accuracy of the landslide susceptibility map (12). Accuracy depends on input data, model accuracy, size of the study area, and experience of professionals. In this study, the ROC curve was applied as a worthy tool for appraising the validation of landslide susceptibility maps derived from the AHP method. The AUC was estimated at 0.817, which meant that the overall success rate of the landslide susceptibility zonation map was 81.7% (Figure 3).

To evaluate the landslide susceptibility map, this map was combined with the landslide inventory map of the study area (Figure 5). The results showed that 0.31%, 4.9%, 12%, 38.3%, and 44.49% of the entire landslide inventory was found

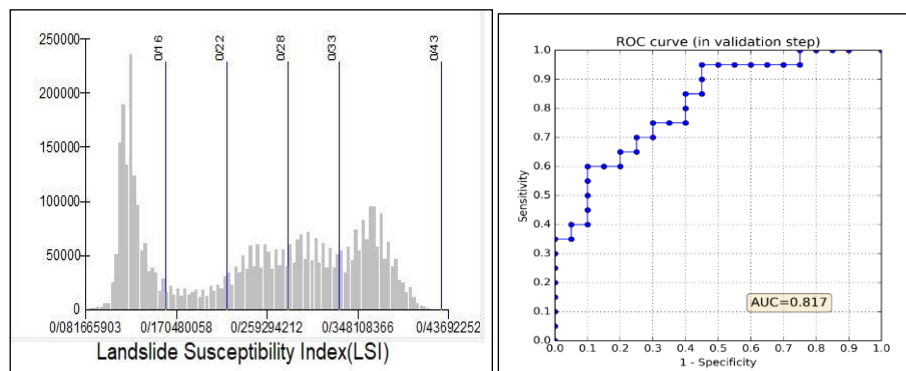


Figure 3. Threshold values for the classification of LSI map and ROC curves of LSM derived from the AHP method (Authors)

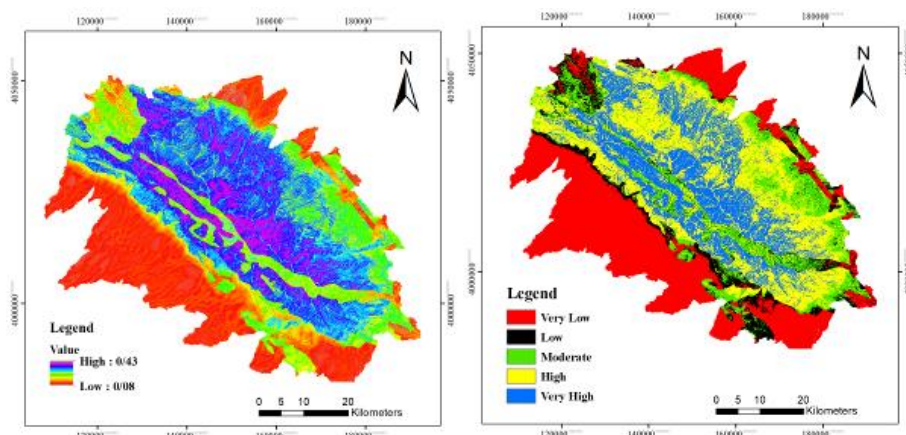


Figure 4. Landslide susceptibility map and landslide susceptibility map of the study area (Authors)

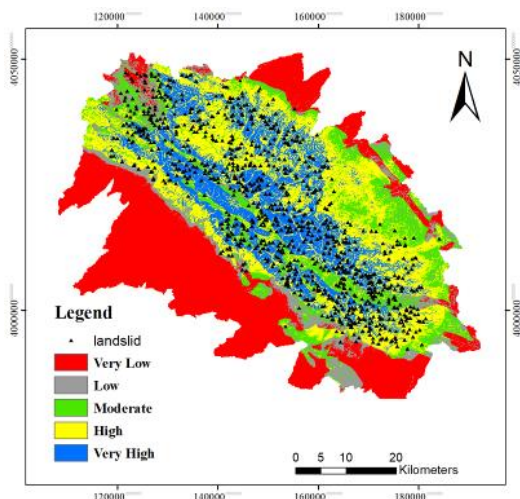


Figure 5. Landslide susceptibility map and landslide inventory map of the study area (Authors)

in the very low, low, moderate, high, and very high susceptibility classes, respectively (Table 5), meaning that landslide susceptibility map had acceptable efficiency.

Table 5. Number and percent of landslide in per class of landslide susceptibility

| Susceptibility classes | Number of landslides | Percent |
|------------------------|----------------------|---------|
| Very low | 3 | 0.31 |
| Low | 47 | 4.9 |
| Moderate | 116 | 12 |
| High | 368 | 38.3 |
| Very high | 427 | 44.49 |

Discussion and Conclusion

Landslide susceptibility mapping is important for visualizing potentially landslide-prone areas in mountainous and hilly terrain (10). This study provided insights into the capability of AHP in predicting landslide susceptible areas. In this regard, 13 triggering factors were considered, including geology aspect, altitude, land use, slope, distance from the road, distance from faults, distance from the river, TPI, TWI, LS, SPI, and annual rainfall. The selection of these 13 factors was based on the availability of data for the study area and the relevance with respect to landslide occurrences. According to the calculation using AHP, the geology was the most influencing data for landslide occurring by the weight of 0.209, then slope, fault, and rainfall by the weights of 0.202, 0.133, and 0.106, respectively. The value of ratio consistency was about 0.08 (less than 0.1),

which showed that the weight was valid and acceptable used in spatial analysis.

Based on the map of landslide susceptibility, 30.9%, 7.9%, 13.4%, 28%, and 19.8% of the entire area were found in the very low, low, moderate, high, and very high susceptibility classes, respectively. According to the findings, very high and high susceptibility classes were observed in the Mayan series formation that consisted of mostly weathered phyllites and shales, which are inherently failure-prone. A similar finding was reported in previous studies (15, 21), according to which geological factor was one of the factors affecting landslides.

In the discussion of slopes, at lower slopes, the force of gravity is less than the resistance forces and at slopes more than 30°, due to climatic conditions and vegetation in Binalood Mountains, soil formation is less. Therefore, in Binalood Mountains most of the highly susceptible areas are observed in 15°-30° slope class. Furthermore, in the study area, high susceptible areas were located in high altitude classes. High altitudes are often rendered unstable by the influence of triggering factors, such as rainfall and earthquakes. Based on iso-rainfall (Figure 2), in the Binalood Mountains, most of the rainfall occurred at high altitudes. According to the results of previous studies (7, 11), altitudes were among the factors affecting landslides. Considering this finding, high and very high susceptibility classes are observed in the north aspect. Since the Binalood Mountains range is located in the northern hemisphere, the north aspect is receiving less sun radiation and high rainfall.

Among the topographic indexes, higher susceptibility classes were reported in the higher SPI and TWI ranges. An increase in TWI ranges boosts water infiltration which often leads to an increase in the pore water pressure and further reduces the soil strength, hence making the terrain prone to slope failures. Stream power index indicates the erosive power of the streams, and higher ranges of SPI are related to the high erosive power of the streams.

Since there are several roads and waterways in Binalood Mountains, it is expected that high susceptibility classes be observed in the areas closer to rivers. This can be attributed to the stream bank erosion which further leads to landslides. Due to slope failure, landslides may occur on the road and the side of the slopes

affected by roads. In this respect, high susceptibility classes are observed in the areas closer to roads. Similar findings were reported in a previous study regarding the effect of roads and waterways on landslides (1). Among the land use classes, bare and very poor woodland areas have high susceptibility.

In the present study, the ROC curve method was used to validate the accuracy of landslide susceptibility map. The results of the present study revealed that the landslide susceptibility map presented good performance in landslide susceptibility assessment (AUC=0.817). In the end, the observed landslide map was overlaid with the landslide susceptibility map. The results of LSM were also found to be matching with the field conditions. Overall, AHP was acceptable for landslide susceptibility mapping in the study area.

The produced LSM in this study can be a good source for decision-makers, planners, and engineers. This map provides valuable information so that attention can be paid to the high and very high susceptible zones for any kind of developmental work.

Acknowledgments

None.

Conflict of Interests

Authors declared no conflict of interests regarding the publication of the present study.

References

- Bahrami Y, Hassani H, Maghsoudi A. Landslide susceptibility mapping using AHP and fuzzy methods in the Gilan province, Iran. *Geo Journal*. 2020; 86: 1797-1816 (In Persian)
- Çellek S. Effect of the slope angle and its classification on landslide. *Natural Hazards and Earth System Sciences Discussions*. 2020; 1-23.
- Chau K, Sze Y, Fung M, Wong W, Fong E, Chan L. Landslide hazard analysis for Hong Kong using landslide inventory and GIS. *Computers & Geosciences*. 2004; 30(4):429-443.
- Chen W, Xie X, Peng J, Shahabi H, Hong H, Bui DT, et al. GIS-based landslide susceptibility evaluation using a novel hybrid integration approach of bivariate statistical based random forest method. *Catena*. 2018; 164:135-149.
- Chen Y, Yu J, Khan S. Spatial sensitivity analysis of multi-criteria weights in GIS-based land suitability evaluation. *Environmental Modelling & Software*. 2010; 25(12):1582-1591.
- Fell R, Corominas J, Bonnard C, Cascini L, Leroi E, Savage WZ. Guidelines for landslide susceptibility, hazard, and risk zoning for land-use planning. *Engineering Geology*. 2008; 102(3-4):99-111.
- Flentje P, Chowdhury R. Resilience and sustainability in the management of landslides. In: *Proceedings of the Institution of Civil Engineers-Engineering Sustainability*. Thomas Telford Ltd; 2016.
- Golovko D, Roessner S, Behling R, Wetzel HU, Kleinschmit B. Evaluation of remote-sensing-based landslide inventories for hazard assessment in Southern Kyrgyzstan. *Remote Sensing*. 2017; 9:943.
- Hong H, Liu J, Bui DT, Pradhan B, Acharya TD, Pham BT, Zhu AX, Chen W, Ahmad BB. Landslide susceptibility mapping using J48 decision tree with AdaBoost, bagging, and rotation forest ensembles in the Guangchang area (China). *Catena*. 2018; 163:399-413.
- Juliev M, Mergili M, Mondal I, Nurtaev B, Pulatov A, Hübl J. Comparative analysis of statistical methods for landslide susceptibility mapping in the Bostanlik District, Uzbekistan. *Science of the Total Environment*. 2019; 653:801-814.
- Kayastha P, Dhital MR, De Smedt F. Application of the analytical hierarchy process (AHP) for landslide susceptibility mapping: A case study from the Tinau watershed, west Nepal. *Computers & Geosciences*. 2013; 52:398-408.
- Kumar R, Anbalagan R. Landslide susceptibility mapping using analytical hierarchy process (AHP) in Tehri reservoir rim region, Uttarakhand. *Journal of the Geological Society of India*. 2016; 87(3):271-286.
- Mandal B, Mandal S. Analytical hierarchy process (AHP) based landslide susceptibility mapping of Lish river basin of eastern Darjeeling Himalaya, India. *Advances in Space Research*. 2018; 62(11): 3114-3132.
- Nguyen TTN, Liu CC. A new approach using AHP to generate landslide susceptibility maps in the Chen-Yu-Lan Watershed, Taiwan. *Sensors*. 2019; 19(3):505.
- Ozer B, Mutlu B, Nefeslioglu H, Sezer E, Rouai M, Dekayir A, Gokceoglu C. On the use of hierarchical fuzzy inference systems (HFIS) in expert-based landslide susceptibility mapping: the central part of the Rif Mountains (Morocco). *Bulletin of Engineering Geology and the Environment*. 2019; 79(3):1-18.
- Panchal S, Shrivastava AK. Application of analytic hierarchy process in landslide susceptibility mapping at regional scale in GIS environment. *Journal of Statistics and Management Systems*. 2020; 23(2):199-206.
- Pourghasemi HR, Pradhan B, Gokceoglu C, Moezzi KD. Landslide susceptibility mapping

- using a spatial multi criteria evaluation model at Haraz Watershed, Iran. In *Terrigenous mass movements*. Springer, Berlin, Heidelberg; 2012; pp. 23-49(In Persian)
18. Pourghasemi HR, Teymouri Yansari Z, Panagos P, Pradhan B. Analysis and evaluation of landslide susceptibility: a review on articles published during 2005–2016 (periods of 2005–2012 and 2013–2016). *Arabian Journal of Geosciences*. 2018; 11:193. (In Persian)
 19. Saleem N, Huq M, Twumasi NYD, Javed A, Sajjad A. Parameters derived from and/or used with digital elevation models (DEMs) for landslide susceptibility mapping and landslide risk assessment: a review. *ISPRS International Journal of Geo-Information*. 2019;8(12):545.
 20. Shahabi H, Hashim M. Landslide susceptibility mapping using GIS-based statically models and remote sensing data in tropical environment. *Scientific Reports*. 2015; 5:8999. (In Persian)
 21. Tsangaratos P, Ilia I, Hong H, Chen W, Xu C. Applying information theory and GIS-based quantitative methods to produce landslide susceptibility maps in Nanchang County, China. *Landslides*. 2017;14:1091-1111.
 22. Wang Y, Fang Z, Wang M, Peng L, Hong H. Comparative study of landslide susceptibility mapping with different recurrent neural networks. *Computers & Geosciences*. 2020; 138:104445.
 23. Wu Y, Li W, Wang Q, Liu Q, Yang D, Xing M, Pei Y, Yan S. Landslide susceptibility assessment using frequency ratio, statistical index, and certainty factor models for the Gangu County, China. *Arabian Journal of Geosciences*. 2016; 9(2).
 24. Zomorodian MJ, Boroumand R. Morphogeno analysis of qualitative and quantitative differences of alluvial cones of Binaloud Mountains with Hydromorphotectonic approach. *Quantitative Geomorphological Researches*. 2013;1(2):53. (In Persian)